

## ELECTROCHEMICAL STUDY OF THE FIRST LAYERS OF OXIDE FORMED ON COPPER IN CARBONATE - BICARBONATE SOLUTIONS

Ribotta, S.B.; Folquer, M.E.\*; Gassa, L.M.<sup>1</sup>

Instituto de Química Física, Facultad de Bioquímica, Química y Farmacia, Universidad Nacional de Tucumán, Ayacucho 491, (4000) San Miguel de Tucumán, Argentina. Tel.: +54-381-424-8170. e-mail: folquer@unt.edu.ar

<sup>1</sup>INIFTA, Facultad de Ciencias Exactas, Universidad Nacional de La Plata, Suc. 4, C.C. 16, (1900) La Plata, Argentina.

*Received May 8, 2003. Accepted in Final Form May 28, 2003*

*Dedicated to Professor Dr. A.J. Arvia on occasion of his 75<sup>th</sup> Anniversary*

### Abstract

*The electrochemical behavior of copper electrodes in different carbonate bicarbonate solutions, with emphasis in the potential region of Cu(I) oxide electroformation and electro-reduction has been studied by voltammetric techniques, scanning electron microscopy (SEM) and electrochemical impedance spectroscopy (EIS). The occurrence of both chemical surface transformations and dissolution processes involving the species formed during the electrochemical reaction are reported. The open circuit experiments reveal the stability of Cu<sub>2</sub>O in spite of the presence of bicarbonate as the aggressive ion. SEM micrographs of the electrode surface allow the characteristics of the different surface products to be distinguished. Capacitance values obtained by EIS reflect the porous nature of the first oxide film electroformed.*

### Resumen

*El comportamiento electroquímico de electrodos de cobre en diferentes soluciones de bicarbonato-carbonato, con énfasis en la región de potencial de electroformación y de electro-reducción de óxido de Cu(I), ha sido estudiado por técnicas voltamétricas, microscopía electrónica de barrido (SEM) y espectroscopia de impedancia electroquímica (EIS). Se informa la ocurrencia de transformaciones químicas superficiales y de procesos de disolución involucrando las especies formadas durante la reacción electroquímica. Los experimentos a circuito abierto revelan la estabilidad del Cu<sub>2</sub>O, a pesar de la presencia del bicarbonato como el ion agresivo. Las microfotografías SEM de la superficie del electrodo permiten distinguir las características de los diferentes productos superficiales. Los valores de capacidad obtenidos por EIS reflejan la naturaleza porosa de la película del primer óxido electroformado.*

### Introduction

The electrochemical behavior of copper in aqueous solutions containing different compositions of carbonate and bicarbonate ions has been studied in different conditions [1-7]. There is a general agreement that initially a porous prepassive film of Cu<sub>2</sub>O is formed followed by an outer layer, composed by CuO/Cu(OH)<sub>2</sub> as in plain sodium

hydroxide solutions [8-19]. A gradual change of the outer layer leads to a complex passive layer composed of basic copper carbonates [5,7,20,21]. It has also been found that the passive layer formation also involves the appearance of Cu(I) and Cu(II) soluble species [2,22-24]. Besides, it has been proved that the presence of bicarbonate does not interfere with the  $\text{Cu}_2\text{O}$  film formation [5].

Although many authors have reported studies about the formation of oxides and passive films, some finer details of the first product formation in the anodic oxidation of copper still remain unfinished. Therefore, it is interesting both from the fundamental and practical standpoint to encourage new measurements in order to confirm previous results reported in the literature.

The aim of this work is to present results of the electrochemical behavior of copper electrodes in different carbonate-bicarbonate buffer solutions with emphasis in the potential range of Cu(I) oxide electroformation and electro-reduction by using voltammetric measurements, open circuit experiments and scanning electron microscopy. Further information was gained using electrochemical impedance spectroscopy.

## Experimental

Measurements were performed in a conventional three-compartment cell. High purity polycrystalline copper rotating discs (Johnson Matthey Chemicals,  $0.15 \text{ cm}^2$  apparent area) embedded in PTFE holders were used as the working electrodes. A large area platinum sheet was used as the counter electrode and a saturated calomel electrode (SCE) was the reference electrode with a Habber-Luggin capillary tip. Electrolyte solutions consisted of a mixture of  $0.75 \text{ M KHCO}_3 + y \text{ M K}_2\text{CO}_3$  ( $0.005 \leq y \leq 0.15$ );  $8.3 \leq \text{pH} \leq 9.5$  and ionic strength (I) between 0.38 and 1.20. They were prepared from analytical grade reagents and threefold distilled water previously boiled to remove  $\text{CO}_2$ . Experiments were made at  $25 \text{ }^\circ\text{C}$  under purified nitrogen gas saturation. Voltammograms were recorded for still electrodes by employing single (STPS) and repetitive (RTPS) triangular potential sweeps between preset cathodic ( $E_{s,c}$ ) and anodic ( $E_{s,a}$ ) switching potentials at a potential scan rate of  $0.025 \text{ V s}^{-1}$ . Impedance measurements (EIS) in the frequency range  $65 \text{ kHz} \geq f \geq 2 \text{ mHz}$ , with  $f = \omega / 2\pi$ , were obtained using a Zahner IM6, at operational potentials between  $-0.300 \text{ V}$  and  $-0.070 \text{ V}$ . Scanning electron microscopy (SEM) was performed using a JEOL-JSM-35CF scanning electron microscope.

## Results and discussion

### *Voltammetric Measurements*

Figure 1 shows a typical voltammogram of copper in still  $0.75 \text{ M KHCO}_3 + 0.05 \text{ M K}_2\text{CO}_3$  solution,  $\text{pH } 8.9$ ,  $I = 0.9$ , run between  $E_{s,c} = -1.300 \text{ V}$  and  $E_{s,a} = 0.300 \text{ V}$  at  $v = 0.025 \text{ V s}^{-1}$ . The positive-going potential scan exhibits three anodic current contributions at  $\sim -0.200 \text{ V}$  and  $\sim 0.040 \text{ V}$  (Peaks 1 and 2, respectively) and a broad potential region with a threshold potential at  $\sim 0.070 \text{ V}$  (Region 3). Peak 1 can be associated to the  $\text{Cu}_2\text{O}$  formation, Peak 2 has been attributed to  $\text{Cu}(\text{OH})_2\text{-CuO}$  complex layer formation and Region 3 has been related to a protective basic copper carbonate layer. The reverse scan presents three cathodic contributions with complex contours in the  $-0.200 \text{ V}$  to  $-0.250 \text{ V}$  potential region (Peak 4),  $-0.650 \text{ V}$  to  $-0.750 \text{ V}$  potential region (Peak 5) and at ca.  $-0.950$

V (Peak 6). Peak 4 has been associated with the electro-reduction of Cu(II) to Cu(I) species [4], Peak 5 has been related to the electroreduction of the basic copper carbonate layer [7,21] and Peak 6 has been assigned to the electro-reduction of the Cu(I) species to Cu(0) [7]. During the anodization of copper in neutral and alkaline solutions both soluble Cu(I) and Cu(II) species have been detected.

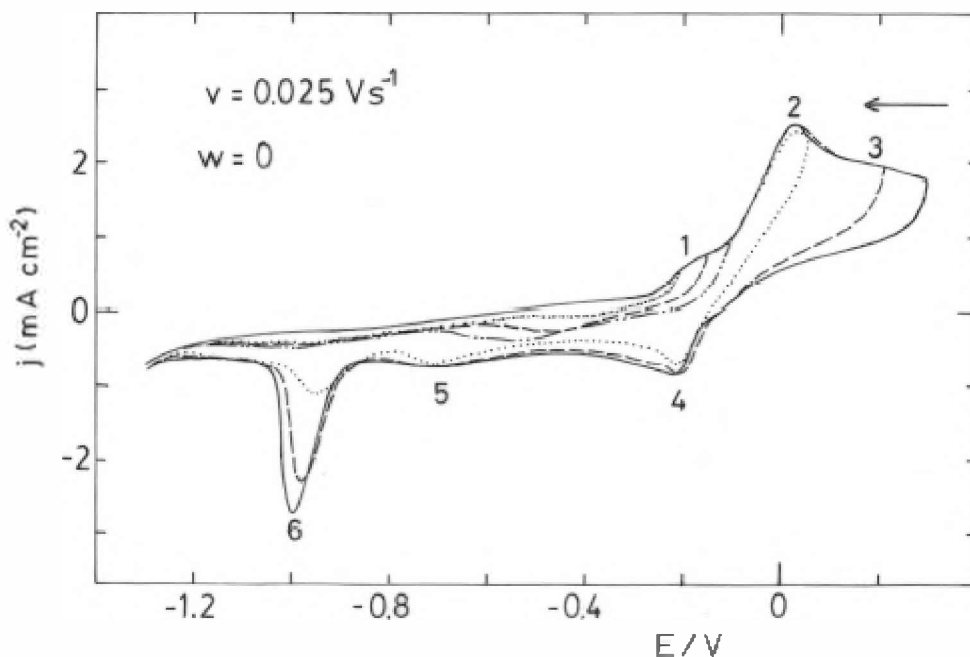


**Figure 1.** Stabilized RTPS  $E/j$  profiles obtained at  $v = 0.025 \text{ V s}^{-1}$  with copper electrode in still  $0.75 \text{ M KHCO}_3 + 0.05 \text{ M K}_2\text{CO}_3$  solution, pH 8.9,  $I = 0.9$ .

When the stabilized voltammogram was obtained, the progressive decrease in  $E_{s,a}$  yield information about the genesis of the multiplicity of the anodic and the cathodic current peaks (Figure 1). Moreover, the general features of the voltammetric response of copper in different  $\text{KHCO}_3 - \text{K}_2\text{CO}_3$  buffers revealed the influence of the pH and the ionic strength of the electrolyte which affect the definition of the various conjugated redox couples (Figure 2).

Apparently, the contribution of anodic Peak 1 could not be distinguished clearly because Peaks 1 and 2 are overlapped (Figures 1 and 2).

The different negative-going potential scans after  $E_{s,a}$  corresponding to the Cu/Cu<sub>2</sub>O potential region indicate that the overall reduction of the Cu(I) species anodically formed is a complex process. At constant potential scan rate the height and the charge density of Peak 6 depend on  $E_{s,a}$  and on the ionic strength of the buffer (Figures 1 and 2). Therefore, the appearance of Peak 6 as  $E_{s,a}$  increases (results not shown but they could be inferred from Figure 1) shows that the anodic oxidation of Cu to Cu(I) ascribed to the potential range of Peak 1 probably involves several species of different reactivity. On the other hand, as the ionic strength of the electrolyte was increased, the whole voltammetric

anodic charge increases, and accordingly, the relative current contribution of Peak 6 increased (Figure 2). These results were related to the formation of soluble corrosion products resulting from the dissolution of Cu(I) and Cu(II) species [18,22]. Besides, bicarbonate behaved as the aggressive ion but with increasing solution pH, an additional factor that affected the dissolution processes seemed to be the local pH value at the reaction interface [20].

However, due to the complex nature of the electrochemical processes involved it is difficult to uncouple them completely.

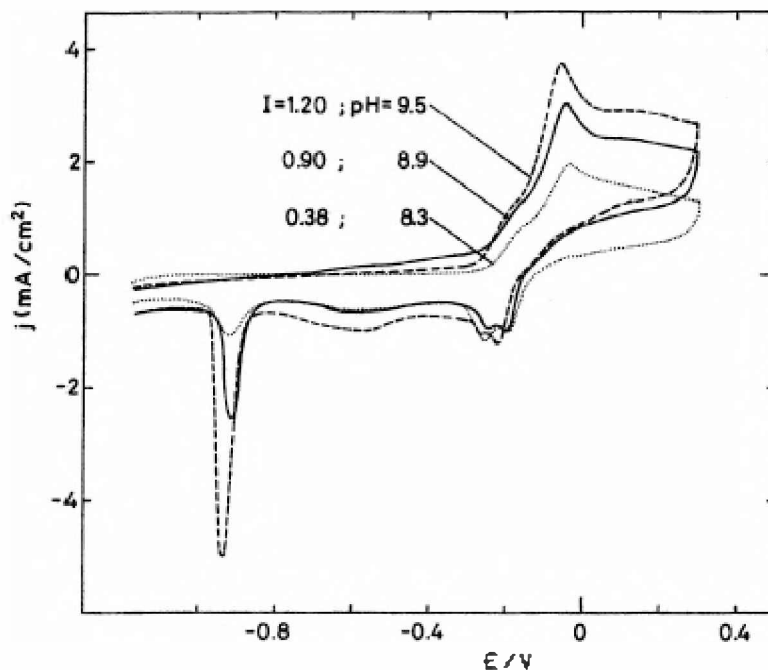


**Figure 2:** Influence of the pH and the ionic strength of the electrolyte on STPS  $E/j$  profiles obtained at  $v = 0.025 \text{ V s}^{-1}$  with copper electrode in still  $0.75 \text{ M KHCO}_3 + y \text{ M K}_2\text{CO}_3$  solutions. (---)  $y = 0.15 \text{ M}$ ; (—)  $y = 0.05 \text{ M}$ ; (...)  $y = 0.005 \text{ M}$ .

### Open Circuit Experiments

The potential transients under open circuit from  $E_{s,c}$  resulting from a STPS voltammogram are independent of  $E_{s,a}$  (Figure 3). When the open circuit potential was measured, the rest potential of the Cu(0)/Cu(I) redox couple was approached. Besides, the limiting open circuit potential was close to the potential of the anodic current Peak 1 ( $E_{P1}$ ) related to the  $\text{Cu}_2\text{O}$  formation (Figure 1).

However, a complex potential decay is shown where two relatively poorly defined transition times are apparently observed. The existence of different oxygen-containing copper species is also deduced and they should be related to the values of the arrest potentials. The first arrest potential obtained is practically the same for the three situations (ca.  $-0.550 \text{ V}$ ) and the final rest potential, already analyzed, was ca.  $-0.280 \text{ V}$ . These results reveal the stability of the first oxide,  $\text{Cu}_2\text{O}$ , formed on the surface electrode.

### SEM Examination

Figures 4 to 7 show SEM micrographs for copper surfaces formed in different experimental conditions. Prior to the experiments, the copper specimens were polarized cathodically at  $E_{s,c} = -1.300$  V for 3 min to obtain a reproducible electro-reduced metal surface. Then, a linear potential sweep at  $v = 0.025$  V s<sup>-1</sup> was applied up to  $E_{s,a}$  set in the potential range of Peak 1 or Peak 2 ( $E_{P1}$  or  $E_{P2}$ ), and finally a potential holding was set at the selected  $E_{s,a}$  for 10 min.

SEM micrographs show considerable differences in the characteristics and distribution of surface products whether the examinations were performed at  $E_{P1}$  (Figure 4) or at  $E_{P2}$  (Figure 5) or at a potential prior to the beginning of the cathodic current Peak 6 (ca. -0.850 V) in the reverse potential scan after the potential holding was set at  $E_{P1}$  (Figure 6) or at  $E_{P2}$  (Figure 7).

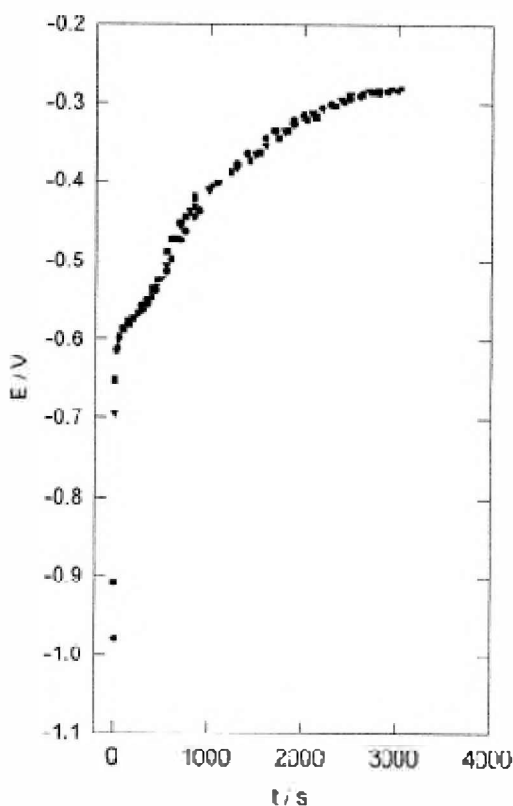


**Figure 3:** Potential transients under open circuit conditions resulting from  $E_{s,c}$  after obtaining the STPS  $E/j$  profiles. Influence of  $E_{s,a}$  at constant electrolyte composition: 0.75 M  $\text{KHCO}_3$  + 0.05 M  $\text{K}_2\text{CO}_3$ , pH 8.9. (●)  $E_{s,a} = E_{P1}$ ; (■)  $E_{s,a} = E_{P2}$ ; (▼)  $E_{s,a} =$  threshold potential of anodic current Peak 1.

A poorly crystallized discontinuous layer of corrosion products formed on the surface was obtained at  $E_{P1}$  (Figure 4[a] through [c]), whereas at  $E_{P2}$  the film showed isolated crystals on a thick porous base film (Figure 5[a] through [c]). Figure 6 shows large isolated crystals surrounded with small needlelike crystals on a porous film, while Figure 7 exhibits a surface completely covered with a high population of small crystals.

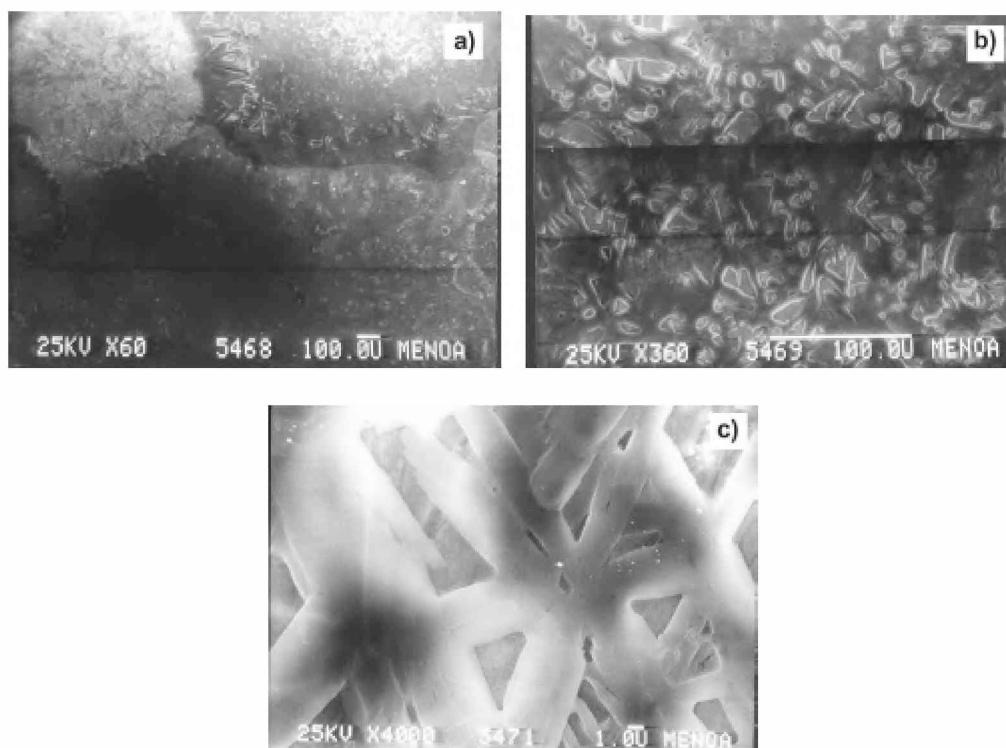


**Figure 4:** SEM micrographs of polycrystalline copper specimens after potential holding for 10 min at the maximum of anodic Peak 1 in still  $0.75\text{ M KHCO}_3 + 0.05\text{ M K}_2\text{CO}_3$ ,  $\text{pH } 8.9$ ,  $I = 0.9$ .

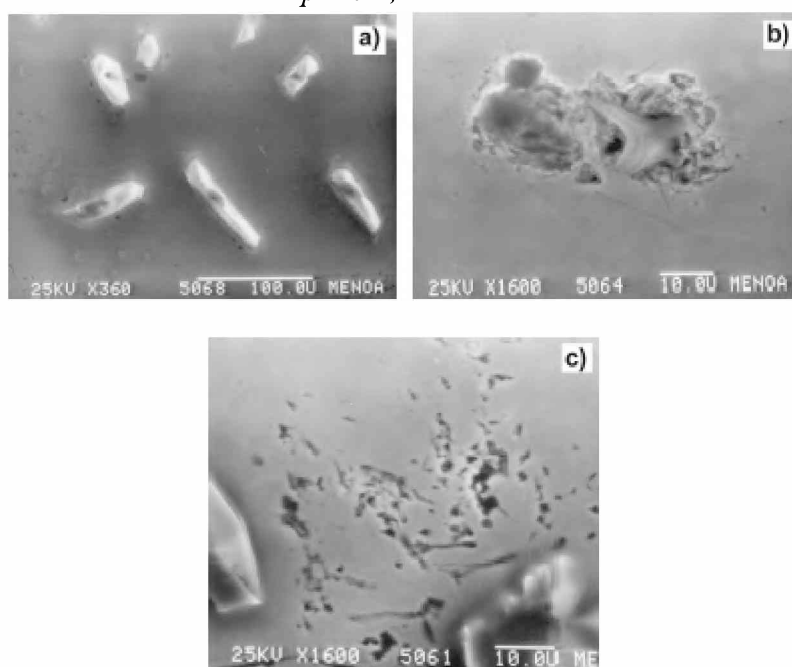


**Figure 5:** SEM micrographs of polycrystalline copper specimens after potential holding for 10 min at the maximum of anodic Peak 2 in still  $0.75\text{ M KHCO}_3 + 0.05\text{ M K}_2\text{CO}_3$  solution,  $\text{pH } 8.9$ ,  $I = 0.9$ .

SEM observations resulting after holding the potential at  $E_{P1}$  or at  $E_{P2}$  suggest that the formation of minor quantities of Cu(II) and basic copper carbonate species, respectively, cannot be disregarded, because the beginning of the Cu(I)  $\rightarrow$  Cu(II) reaction is overlapped by the end of Cu(0)  $\rightarrow$  Cu(I) reaction and similarly, the first reaction by the beginning of the basic copper carbonates formation reaction (Figure 1). On the other hand, the potential holding promote possible chemical surface transformations of the anodic species [10].

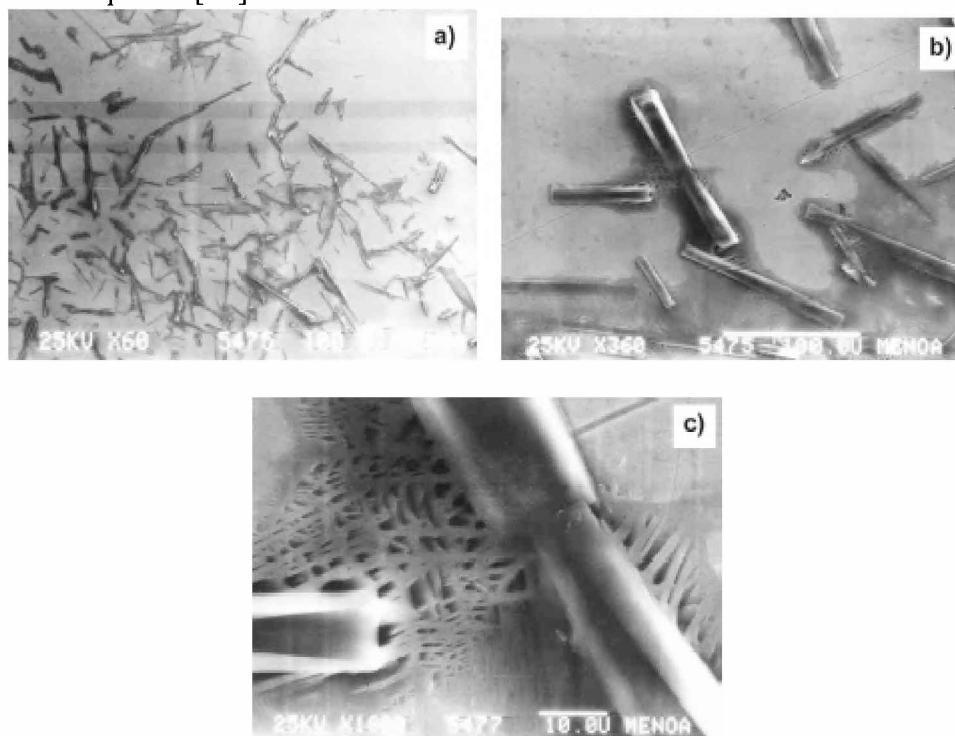


**Figure 6:** SEM micrographs of polycrystalline copper specimens at ca.  $-0.850 V$  (potentiostatically formed during 10 min at  $E_{P1}$ ) in still  $0.75 M KHCO_3 + 0.05 M K_2CO_3$  solution, pH 8.9,  $I = 0.9$ .

The differences observed in SEM results obtained at a potential prior to the beginning of Peak 6 (Figures 6 and 7) indicate that the thickness and the general characteristics of the  $Cu_2O$  layer formed is strongly influenced by the time interval spent between the anodic and the cathodic processes and by the subsequent different transformations involving the species formed during the electrochemical reaction [22].

#### EIS Data

Figures 8[a] through [c] show the Nyquist diagrams for copper in the stagnant  $0.75 M KHCO_3 + 0.05 M K_2CO_3$  solution, pH 8.9,  $I = 0.9$ . Impedance spectra at different applied potentials exhibit two slightly distorted capacitive semicircles. Deviations from the ideal semicircles can be attributed to inhomogeneities of the surface [25].

The general features of the frequency response of the Cu electrodisolution reaction at comparable potentials in different carbonate-bicarbonate buffers do not differ

significantly, but real and imaginary components of the impedance decrease with increasing ionic strength (Figures 8 and 9).

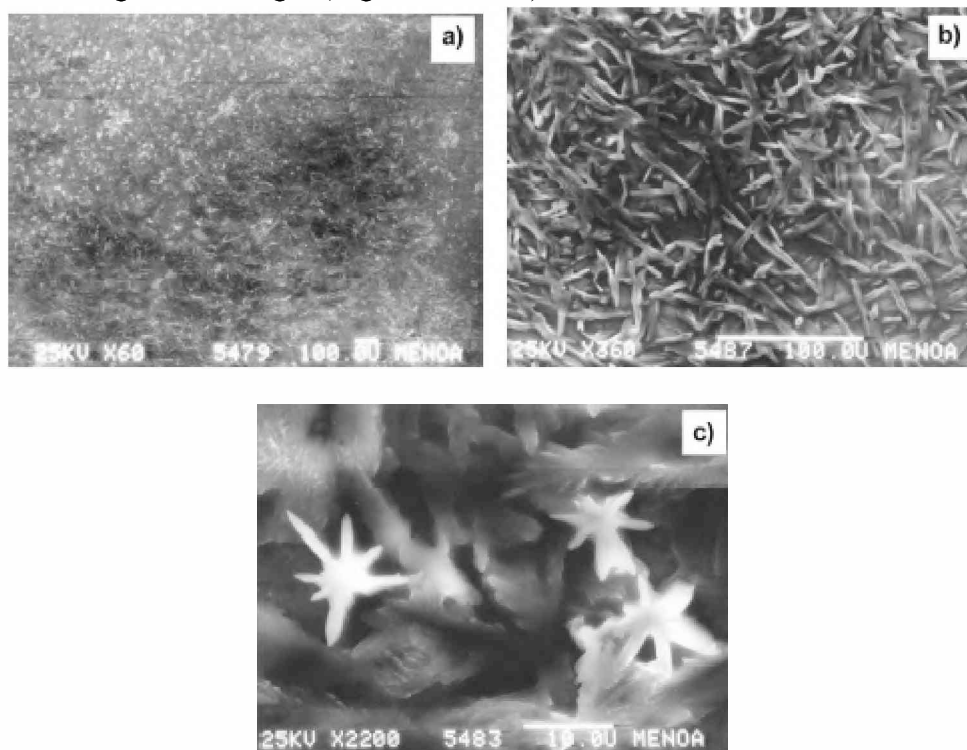


**Figure 7:** SEM micrographs of polycrystalline copper specimens at ca.  $-0.850\text{ V}$  (potentiostatically formed during 10 min at  $E_{P_2}$ ) in still  $0.75\text{ M KHCO}_3 + 0.05\text{ M K}_2\text{CO}_3$  solution, pH 8.9,  $I = 0.9$ .

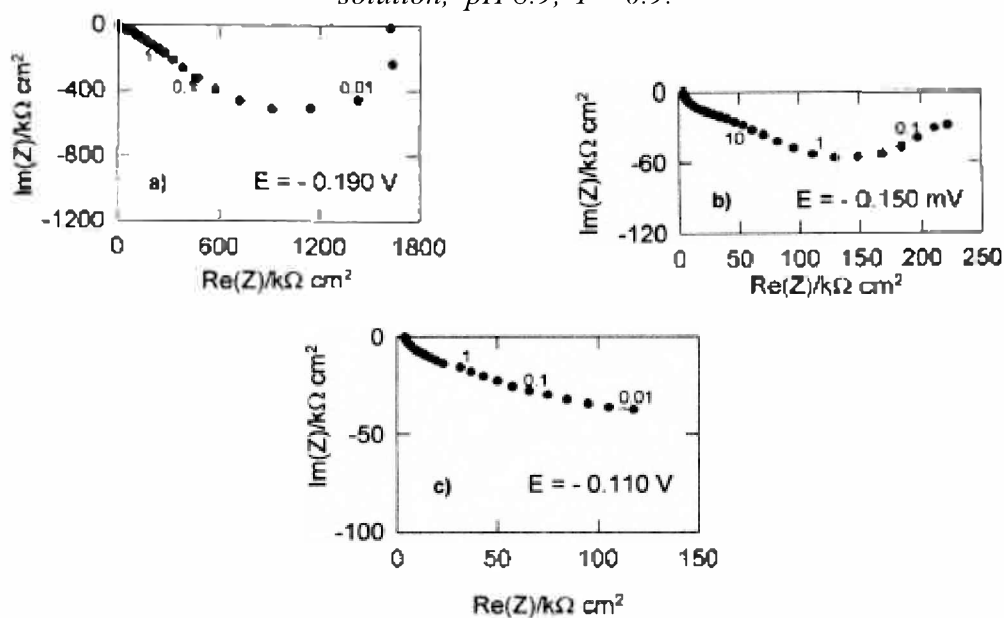


**Figure 8:** Nyquist plots for Cu in still  $0.75\text{ M KHCO}_3 + 0.05\text{ M K}_2\text{CO}_3$  solution, pH 8.9,  $I = 0.9$ .

From the optimum fitting results, the low capacitance values obtained ( $8 \pm 5 \mu\text{F cm}^{-2}$ ) may be associated to a  $\text{Cu}_2\text{O}$  film [26], with an empirical exponent,  $\alpha \approx 0.84$ , indicating it is a porous film, as it was observed by SEM (Figures 4[a] through [c]). The low capacitance values are in good agreement with typical values of a metal covered by a passive film [27].

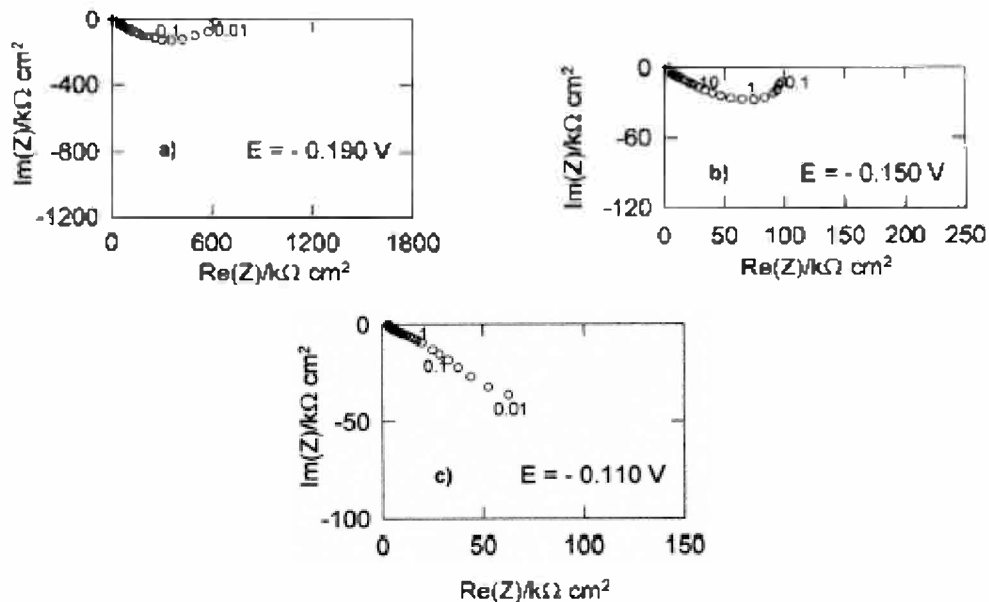


**Figure 9:** Nyquist plots for Cu in still  $0.75 \text{ M KHCO}_3 + 0.15 \text{ M K}_2\text{CO}_3$  solution, pH 9.5,  $I = 1.2$ .

## Conclusions

The electrochemical response of copper ion bicarbonate-carbonate solutions ( $8.3 \leq \text{pH} \leq 9.5$ ) depends on pH, ionic strength of the electrolyte and the potential window studied.

The film formation in the potential region corresponding to the oxidation of  $\text{Cu}(0)$  to  $\text{Cu}(I)$  probably involves several species of different reactivity. Dissolution processes of oxide  $\text{Cu}(I)$  and  $\text{Cu}(II)$  species also take place. Thus, the electro-reduction sequence of the first layers of oxide is a composite process.

The potential transients under open circuit from  $E_{s,c}$  confirm the existence of different oxygen-containing copper species and reveal the stability of  $\text{Cu}_2\text{O}$ .

EIS data give low capacitance values associated to a  $\text{Cu}_2\text{O}$  layer indicating it is a porous film.

SEM micrographs contribute to distinguish the different surface products formed under well-controlled conditions.

## Acknowledgments

This research has been supported by Consejo Nacional de Investigaciones Científicas y Técnicas and Consejo de Investigaciones de la Universidad Nacional de Tucumán. The authors acknowledge the assistance of A. Andrada Barone with the SEM micrographs.

## References

- [1] Duby, P. *The Thermodynamic Properties of Aqueous Inorganic Copper Systems*, International Copper Research Association NSRDS, NBS, **1977**.
- [2] Vásquez Moll, D.; G. de Chialvo, M.R.; Salvarezza, R.C.; Arvía, A.J. *Electrochim. Acta*, **1985**, *30*, 1011.
- [3] Di Quarto, F.; Piazza, S.; Sunseri, C. *Electrochim. Acta*, **1985**, *30*, 315.
- [4] Pérez Sánchez, M.; Barrera, M.; González, S.; Souto, R.M.; Salvarezza, R.C.; Arvía, A.J. *Electrochim. Acta*, **1990**, *35*, 1337.
- [5] Drogowska, M.; Brossard, L.; Ménard, H. *J. Electrochem. Soc.*, **1992**, *139*, 39.
- [6] Drogowska, M.; Brossard, L.; Ménard, H. *J. Electrochem. Soc.*, **1993**, *140*, 1247.
- [7] Pérez Sánchez, M.; Souto, R.M.; Barrera, M.; González, S.; Salvarezza, R.C.; Arvía, A.J. *Electrochim. Acta*, **1993**, *38*, 703.
- [8] Shoesmith, D.W.; Rummery, T.E.; Owen, D.; Lee, W. *J. Electrochem. Soc.*, **1976**, *123*, 790.
- [9] Strehblow, H.-H.; Titze, B. *Electrochim. Acta*, **1980**, *25*, 839.
- [10] Marchiano, S.L.; Elsner, C.I.; Arvía, A.J. *J. Appl. Electrochem.*, **1980**, *10*, 365.
- [11] Strehblow, H.-H.; Speckmann, H.-D. *Werkst. Korros.*, **1984**, *35*, 512.
- [12] G. de Chialvo, M.R.; Marchiano, S.L.; Arvía, A.J. *J. Appl. Electrochem.*, **1984**, *14*, 165.
- [13] Speckmann, H.-D.; Lohrengel, M.M.; Schultze, J.W.; Strehblow, H.-H. *Ber. Bunsenges. Phys. Chem.*, **1985**, *89*, 392.
- [14] G. de Chialvo, M.R.; Salvarezza, R.C.; Vásquez Moll, D.; Arvía, A.J. *Electrochim. Acta*, **1985**, *30*, 1501.
- [15] Pyun, C.-H.; Park, S.-M. *J. Electrochem. Soc.*, **1986**, *133*, 2024.
- [16] Figueroa, M.G.; Salvarezza, R.C.; Arvía, A.J. *Electrochim. Acta*, **1986**, *31*, 665.
- [17] Collisi, U.; Strehblow, H.-H. *J. Electroanal. Chem.*, **1990**, *284*, 385.
- [18] Dong, S.; Xie, Y.; Cheng, G. *Electrochim. Acta*, **1992**, *37*, 17.
- [19] Drogowska, M.; Brossard, L.; Ménard, H. *J. Appl. Electrochem.*, **1994**, *24*, 344.
- [20] Ribotta, S.B.; Folquer, M.E.; Vilche, J.R. *Corrosion*, **1995**, *51*, 682.
- [21] Van Muylder, J. In *Comprehensive Treatise of Electrochemistry*, Vol. 4; eds. Bockris, O'M.; Conway, B.E.; Yeager, E.; White, R.E.; Plenum Press: New York, **1981**; p. 1-96.
- [22] Castro Luna de Medina, A.M.; Marchiano, S.L.; Arvía, A.J. *J. Appl. Electrochem.*, **1978**, *8*, 121.
- [23] Gómez Becerra, J.; Salvarezza, R.C.; Arvía, A.J. *Electrochim. Acta*, **1988**, *33*, 613.
- [24] Zhou, A.; He, D.; Xie, N.; Xie, Q.; Nie, L.; Yao, S. *Electrochim. Acta*, **2000**, *45*, 3943.
- [25] Jüttner, K. *Electrochim. Acta*, **1990**, *35*, 1501.
- [26] Ribotta, S.B.; Folquer, M.E.; Real, S.G.; Gassa, L.M. *Corrosion*, **2002**, *58*, 240.
- [27] Simões, A.M.P.; Ferreira, M.G.S.; Rondot, B.; da Cunha Belo, M. *J. Electrochem. Soc.*, **1990**, *137*, 82.